EVALUATION OF RELATIVE NAVIGATION ALGORITHMS FOR FORMATION-FLYING SATELLITES

David Kelbel, Taesul Lee, and Anne Long
Computer Sciences Corporation
Lanham-Seabrook, Maryland USA 20706

J. Russell Carpenter and Cheryl Gramling
NASA Goddard Space Flight Center
Greenbelt, Maryland USA 20771

ABSTRACT

Goddard Space Flight Center is currently developing advanced spacecraft systems to provide autonomous navigation and control of formation flyers. This paper discusses autonomous relative navigation performance for formations in eccentric, medium and high altitude Earth-orbits using Global Positioning System (GPS) Standard Positioning Service (SPS) and intersatellite range measurements. The performance of several candidate relative navigation approaches is evaluated. These analyses indicate that the relative navigation accuracy is primarily a function of the frequency of acquisition and tracking of the GPS signals. A relative navigation position accuracy of 0.5 meters root-mean-square (RMS) can be achieved for formations in medium-attitude eccentric orbits that can continuously track at least one GPS signal. A relative navigation position accuracy of better than 75 meters RMS can be achieved for formations in high-altitude eccentric orbits that have sparse tracking of the GPS signals. The addition of round-trip intersatellite range measurements can significantly improve relative navigation accuracy for formations with sparse tracking of the GPS signals.

1 – INTRODUCTION

Formation-flying techniques and satellite autonomy will revolutionize space and Earth science missions and enable many small, inexpensive satellites to fly in formation and gather concurrent science data. The Guidance, Navigation, and Control Center (GNCC) at Goddard Space Flight Center (GSFC) has successfully developed high-accuracy autonomous satellite navigation systems using the National Aeronautics and Space Administration's (NASA's) space and ground communications systems and the Global Positioning System (GPS) (References 1 and 2). Recently, the GNCC has leveraged this experience to develop advanced spacecraft systems that provide autonomous navigation and control of formation flyers.

To support this effort, the GNCC is assessing the relative navigation accuracy achievable for proposed formations using GPS and intersatellite range measurements. Several universities and corporations are developing GPS transceivers that support this tracking concept for NASA and the Air Force Research Laboratory; these include Johns Hopkins Applied Physics Laboratory, International Telephone and Telegraph, Honeywell, Motorola, Jet Propulsion Laboratory, Cincinnati Electronics, and Stanford University (Reference 3). This paper evaluates the performance of several candidate relative navigation algorithms for missions with more than two vehicles maintaining a relatively tight formation, in a relatively eccentric orbit.

High-fidelity simulations were performed to study two proposed formation-flying missions. One is a mission designed to study the Earth's aurora. This medium-altitude formation consists of four satellites maintained in eccentric Earth orbits of approximately 500x7000 kilometer altitudes. To support autonomous planning of the formation-flying maneuvers to maintain the initial 10-kilometer separation at apogee, the total relative position and velocity accuracy must be about 100 meters and 20 millimeters per second, respectively. Later in the mission, when the separation is reduced to about 500 meters, the total relative position accuracy requirement reduces to 5 meters.

The other formation-flying mission is the initial phase of the Magnetospheric Multiscale (MMS) mission. The MMS formation consists of four satellites in eccentric orbits of approximately 1.2x12 Earth radii. The intersatellite separation at apogee varies from 10 kilometers to 0.1 Earth-radii over the life of the mission. The absolute position knowledge requirement is 100 kilometers and the intersatellite position knowledge requirement is 1 percent of the actual separation.

Previously, the authors investigated the relative navigation accuracy that could be achieved for the 500x7000 kilometer formation by differencing independently-estimated state vectors (Reference 4). That analysis indicated that an autonomous relative navigation position accuracy of 1 meter root-mean-square (RMS) can be achieved by differencing high-accuracy filtered solutions if only measurements from common GPS space vehicles (SVs) are used in the independently-estimated solutions. This paper quantifies the relative navigation accuracy improvements achievable using a high-accuracy multi-satellite filter to simultaneously estimate the satellite state vectors. Improvements to be achieved through the estimation of GPS biases, differencing of GPS measurements, and addition of intersatellite range measurements are also evaluated.

2 – RELATIVE NAVIGATION ALGORITHMS

The most straightforward relative navigation approach computes the satellite relative positions by differencing the absolute position vectors of each satellite in the formation. The state differencing method can be used to support decentralized, centralized, or hierarchical formation control strategies. Figure 1 illustrates one possible configuration for using this approach to support decentralized control of a distributed satellite formation. In this case, each satellite independently computes its absolute state vector using GPS and possibly intersatellite measurements and transfers this state vector via an intersatellite communications link to every other satellite in the formation. Each satellite computes its relative position to the other satellites by state vector differencing and uses this relative state to plan and execute formation maintenance maneuvers to maintain its desired position within the formation. Reference 5 discusses a recent investigation of decentralized formation control strategies.

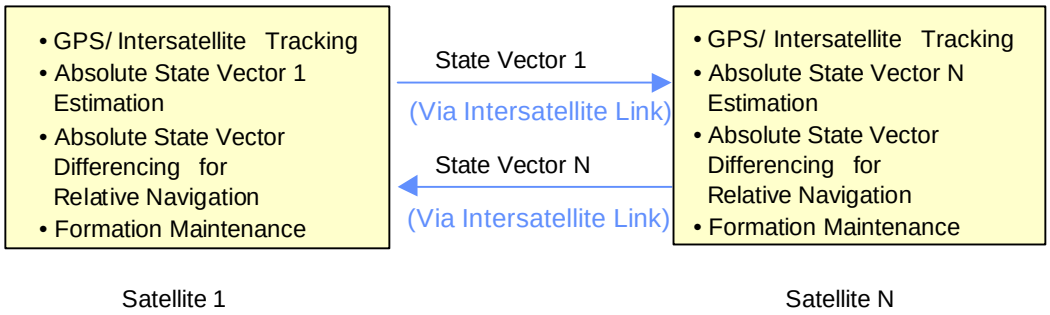

Figure 1. Independent State Vector Differencing Configuration with Decentralized Formation Control

The absolute state vector computation can be performed using either an instantaneous point solution method or a real-time filtered algorithm. The analysis presented in Reference 4 indicates that relative navigation by differencing absolute state vectors obtained using the point solution method is not suitable for continuous real-time navigation of MEO and HEO formations for which fewer than six GPS SVs are visible during significant portions of the orbit. In addition, because point solutions do not provide accurate velocity estimates, they are not suitable for applications in which state vector information must be predicted ahead in time, e.g., to support autonomous maneuver planning.

A real-time filtered algorithm, such as that implemented in the GPS Enhanced Orbit Determination (GEODE) software (Reference 6), reduces the impact of the measurement errors by using an extended Kalman filter in conjunction with a high-fidelity orbital dynamics model. In addition to the differencing of independently-estimated state vectors, the real-time filtered approach can support more complex relative navigation approaches that simultaneously estimate the state vectors of all satellites in the formation. Figure 2 illustrates one possible configuration for using the simultaneous estimation approach to support decentralized control of a distributed satellite formation. In this configuration, each satellite computes the absolute state vectors of all satellites in the formation using GPS measurements to all satellites and possibly intersatellite measurements. Each satellite transfers its GPS measurements via an intersatellite communications link to every other satellite in the formation. Each

satellite computes its relative position to the other satellites by state vector differencing and uses this relative state to plan and execute formation maintenance maneuvers to maintain its desired position within the formation.

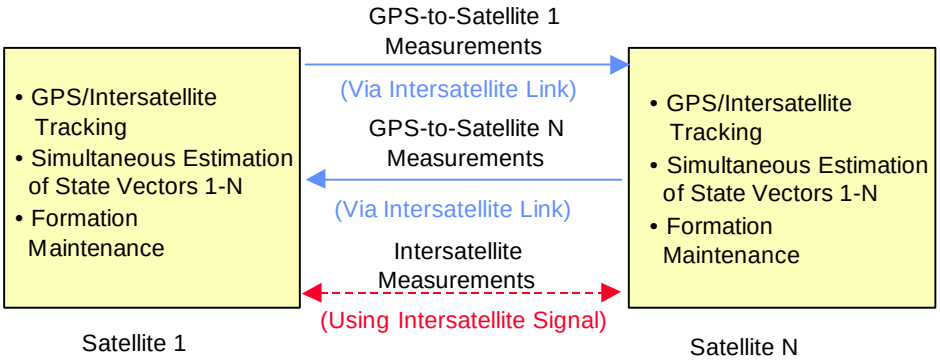

Figure 2. Simultaneous State Vector Estimation Configuration with Decentralized Formation Control

Table 1 lists the characteristics of the navigation algorithms evaluated in this paper. In this table, "local" refers to the satellite on which a specific copy of the navigation software resides. "Remote" refers to the other satellites in the formation. In the decentralized satellite configuration, each satellite hosts the same navigation software but does not necessarily process the same set of measurements.

Table 1. Navigation Algorithms

Navigation Algorithm	Absolute State Vectors Estimated	Measurement Types	Data Transferred From Remotes to Local
Independent	Local satellite	GPS pseudorange to local	Remote satellite state vectors
Simultaneous with standard GPS	Local and remote satellites	GPS pseudorange to local and remotes	GPS measurements for remotes
Simultaneous with standard GPS and bias estimation	Local and remote satellites Random walk measurement biases for each GPS SV	GPS pseudorange to local and remotes	GPS measurements for remotes
Simultaneous with differenced GPS	Local and remote satellites	Singly differenced GPS pseudorange between local and remotes	GPS measurements for remotes
Simultaneous with standard and differenced GPS	Local and remote satellites	GPS pseudorange to the local Singly differenced GPS pseudorange between local and remotes	GPS measurements for remotes
Simultaneous with standard GPS and 1-way intersatellite	Local and remote satellites Random walk measurement biases for each remote to local intersatellite link	GPS pseudorange to local and remotes Intersatellite pseudorange from remote to local	GPS measurements for remotes
Simultaneous with standard GPS and round-trip intersatellite	Local and remote satellites	GPS pseudorange to local and remotes Intersatellite range from local-to-remote-to-local	GPS measurements for remotes

3 – PERFORMANCE SIMULATION PROCEDURE

To quantify the level of relative navigation performance that is achievable for formations in MEO and HEO, realistic simulations were performed for two representative missions. The MEO formation studied consists of four satellites maintained in eccentric Earth orbits at an inclination of 80 degrees with altitudes of approximately 500 kilometers at perigee by 7000 kilometers at apogee. The orbital period is approximately 3 hours. All satellites have nearly identical surface areas of 0.6613 meters^2 and masses of 200 kilograms. The intersatellite separations in

this tetrahedral formation range from 10 kilometers at apogee to 30 kilometers at perigee, with three satellites in the same orbit plane and one out of plane.

The HEO formation consists of four satellites maintained in 1.2-Earth-radii by 12-Earth-radii orbits at an inclination of 10 degrees, which is similar to the formation proposed for the first phase of the Magnetospheric Mapping mission. The orbital period in this mission phase is 1 day. All satellites have nearly identical surface areas of 1.12 meters^2 and masses of 220 kilograms. The intersatellite separations in this tetrahedral formation range from 10 kilometers at apogee to 150 kilometers at perigee, with planar separations of less than 0.1 degree.

3.1 – Measurement Simulation

Realistic GPS pseudorange and remote-to-local and round-trip intersatellite range measurements were simulated for each MEO/HEO satellite using high-fidelity truth ephemerides and the measurement simulation options listed in Table 2. The truth ephemerides were generated using the Goddard Trajectory Determination System (GTDS) with the high-accuracy force model, which included a Joint Goddard Model (JGM) for nonspherical gravity forces, Jet Propulsion Laboratory Definitive Ephemeris 200 for solar and lunar gravitational forces, atmospheric drag, and solar radiation pressure forces. GTDS is the primary orbit determination program used for operational satellite support at GSFC.

Table 2. GPS Measurement Simulation Parameters

Parameter	Value
Measurement data rate	GPS: every 60 seconds from all visible GPS SVs Intersatellite: every 60 seconds from all remote SVs for MEO every 60 seconds from all remote SVs for 10 minutes per hour for HEO
GPS SV ephemerides	Broadcast ephemerides for June 21-26, 1998
GPS SV characteristics:	
Ephemeris and clock errors	2 meter (1-sigma)
Transmitting antenna pattern	GPS L-band pattern, modeled from 0 to 90 degrees down from boresight
Transmitted power	29.8 dB-watts in maximum gain direction
User antenna models:	Hemispherical antenna : Maximum gain : 3.5 dBic for MEO, 4.9 dBic for HEO Horizon mask: 90 degrees from boresight
Visibility constraints	• Earth blockage with 500 km altitude tropospheric mask • GPS SV transmitting antenna beamwidth and receiving antenna horizon masks • Received signal-to-noise ratio above tracking threshold
GPS receiver characteristics	• Receiver noise figure: 2.9 dB for MEO, 4.9 dB for HEO • System noise temperature: Earth-point antenna: 300K Otherwise: 190K • 24-channels • 35 dB-Hertz receiver acquisition threshold for MEO • 30 dB-Hertz receiver acquisition threshold for HEO
Ionospheric delays	MEO: 26 meters at 500 km height 5 meters at 1000 km HEO: 32 meters at 400 km height 3 meters at 1000 km
Receiver clock bias white noise spectral density	9.616×10^{-20} seconds^2 per second
Receiver clock drift rate white noise spectral density	1.043×10^{-27} seconds^2 per seconds^3
Random measurement errors	GPS pseudorange: 2 meters (1-sigma) Intersatellite pseudorange: 2 meters (1-sigma)

The GPS constellation configuration was based on the GPS broadcast messages for the epoch date. The GPS signal strength at the GPS receiver's location was modeled assuming the nominal GPS Block II signal antenna pattern (including both the main and side lobes). Each MEO satellite had one hemispherical GPS antenna, with a zenith-

pointing boresight. The MEO's GPS receiver's signal-to-noise ratio acquisition threshold was 35 dB-hertz, consistent with the performance of most space receivers. Each HEO satellite had identical hemispherical antennas, pointing in the zenith and anti-zenith directions. The HEO formation pseudorange measurements were created based on a GPS receiver with a reduced acquisition threshold of 30 dB-Hertz. The GPS SV signal attenuation model that was used provides realistic signal acquisition predictions (Reference 7). The number of simultaneous measurements was not restricted.

GPS SV ephemeris and clock errors were applied at a 2-meter (1-sigma) level, using the Lear4 autoregressive integrated moving average time series model (Reference 8). When the satellites were below the Earth's ionosphere, ionospheric delays were modeled as a function of the height of the signal path above the Earth, which was based on ionospheric delays computed for the test orbit using the Bent ionospheric model available in GTDS. In the case of signals with long paths "over-the-Earth-limb", ionospheric delays were modeled using an exponential function of the height of ray path (HORP) above the Earth, which was based on ionospheric delays computed for each test orbit using the Bent ionospheric model. Receiver clock noise was simulated assuming a highly-stable crystal oscillator with a 1-second root Allan variance of $0.16(10^{-9})$. A twice-integrated random walk model, which is based on Reference 9, was used to simulate the clock bias and clock drift noise contributions to the GPS and intersatellite measurement errors.

Intersatellite pseudorange measurements have potentially large biases due to the transmitter's and receiver's clock biases. Several strategies could be used to reduce or eliminate these biases. To reduce these biases, each transmitting satellite could estimate its clock offset from GPS time and frequency offset from nominal based on GPS measurements and steer its clock to be synchronized to within 100 nanoseconds (30 m) with GPS time. Summation of the remote-to-local and local-to-remote pseudoranges would cancel the clock bias contributions. Measurement of the round-trip intersatellite range eliminates the clock bias contributions. In the simulations reported in this paper, the remote-to-local (1-way) interstatellite measurements are biased by the difference between the simulated transmitter and receiver clock biases. The simulated round-trip intersatellite measurements are unbiased.

3.2 – Navigation Performance Analysis Procedure

Monte Carlo simulations were performed for each formation to quantify the expected distribution in the absolute and relative solution errors as a function of variations in the random measurement errors. The following ensemble error statistics were accumulated for the ensemble of navigation solutions obtained by processing 25 sets of simulated GPS pseudorange measurements that were created by varying the random number seeds used for the GPS ephemeris and clock, receiver clock, and random measurement errors:

- The ensemble RMS/maximum error, which is the RMS/maximum of the true error (difference between the estimated and the true state) at each time computed across all Monte Carlo solutions.
- The steady-state time-wise ensemble RMS/maximum error, which is the RMS/maximum of the ensemble true errors computed along the time axis, omitting the initial convergence period.

The extended Kalman filter algorithm available in the GEODE flight software was used to process these measurement sets. The filter was "tuned" by adjusting the process noise parameters and measurement standard deviation to produce an estimated state error root variance that was consistent with the ensemble RMS state error obtained in the Monte Carlo analysis. Table 3 lists the GEODE processing parameters common to all cases. Atmospheric drag and solar radiation pressure forces were included in the state propagation using atmospheric drag and solar radiation pressure coefficients that were offset by 10 percent and 5 percent respectively from the values used in the truth ephemeris generation.

The absolute navigation errors were computed by differencing the truth and estimated absolute state vectors. The estimated relative state vectors were computed by differencing the estimated absolute state vectors for the two satellites. The relative navigation errors were computed by differencing the true relative state vectors and the estimated relative state vectors.

Table 3. GEODE Processing Parameters

Parameter	Value
Nonspherical Earth Gravity model	MEO: 30x30 JGM-2 HEO: 8x8 JGM-2
Solar and lunar ephemeris	High-precision analytical ephemeris
Initial position error in each component	100 meters for MEO, 5000 meters for HEO
Initial velocity error in each component	0.1 meter per second
Initial solar radiation pressure coefficient error	0.07 (5 percent)
Atmospheric drag coefficient error	0.22 (10 percent)
Initial receiver time bias error	100 meters
Initial receiver time bias rate error	0.1 meter per second
Estimated state (local and remote satellites)	• position and velocity • GPS receiver time bias and time bias drift • Atmospheric drag coefficient correction (MEO only) • Intersatellite bias with 1-way measurements
GPS SV ephemerides	Broadcast ephemerides for June 21-26, 1998
Ionospheric editing	500 kilometer minimum ray path height

4 – RELATIVE NAVIGATION PERFORMANCE FOR MEDIUM ALTITUDE FORMATION

This section presents the absolute and relative navigation results for the MEO formation. Figure 3 illustrates the geometry of the MEO spacecraft with respect to the primary beam of a single GPS satellite (ignoring the effects of the differences in inclinations). The MEO lies well below the GPS constellation altitude.

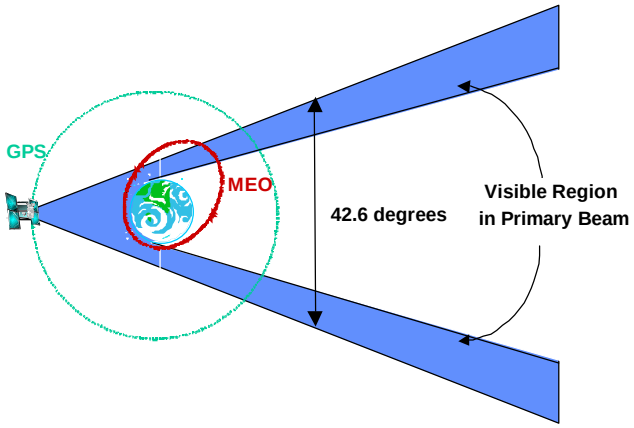

Figure 3. MEO Tracking Geometry

Figure 4 shows the number of GPS SVs visible as a function of time and altitude. The satellite's single zenith-pointing hemispherical antenna considerably limits GPS visibility at high altitudes. The periods of lowest visibility (4 or fewer GPS SVs) occur when the satellites are at altitudes above 5500 kilometers, where the visibility is highly dependent on the exact position of the GPS SVs within each orbit plane. The periods of best visibility with 6 or more visible GPS SVs occur when the satellites are within the main lobe of the GPS signal (i.e. below approximately 3000 kilometers).

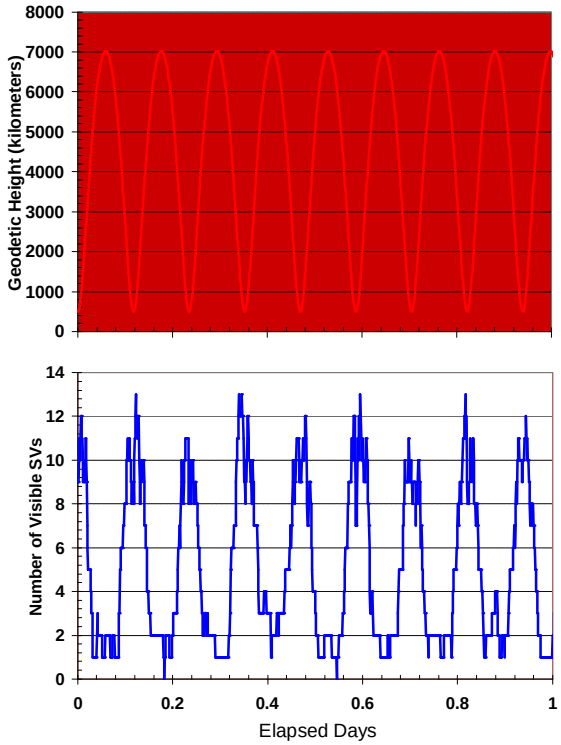

Figure 4. **GPS SV Visibility as a Function Time and Altitude for MEO Formation**

Figure 5 shows the ensemble RMS and maximum absolute position and clock errors for the local satellite over the 2-day estimation time span followed by a 1-day prediction time span, from a Monte Carlo simulation in which all satellites were independently estimated using standard GPS measurements. The estimation process reached steady state after 3 hours of processing, immediately following the second perigee passage. The variation in the absolute and relative error statistics for all satellites in the formation is less than 2 and 3 percent; respectively. The steady-state (i.e., omitting the initial convergence period) time-wise ensemble RMS of the absolute errors were 3.35 meters position, 1.7 millimeters per second velocity, and 8 meters (0.03 microseconds) clock bias, which were very consistent with the state errors predicted by the estimator. The maximum errors occur following apogee. For the Monte Carlo simulation, the maximum absolute errors encountered were less than 9.3 meters, 6.8 millimeters per second velocity, and 26 meters (0.09 microseconds). During a 1-day prediction using a converged filter solution, the absolute errors remain under 17 meters in position, 17 millimeters per second in velocity, and 1412 meters (4.71 microseconds) in clock bias. The primary sources of the absolute navigation error are dynamic modeling errors, unmodeled ionospheric delay, GPS SV ephemeris and clock errors, and receiver clock errors.

Figure 6 shows the ensemble RMS and maximum relative position error for the local satellite and one remote satellite, from the same Monte Carlo simulation. When the absolute solutions are differenced, the error contributions from correlated measurement and dynamic errors cancel and the relative navigation accuracy is significantly better than the absolute errors. Since the satellites are in tight formation in nearly the same orbits, the dynamic errors are highly correlated, and a large percentage of the dynamic error contribution cancels in all of these cases. In addition, since the satellites are in close formation and track common GPS SVs 99.8 percent of the time, the ionospheric delay and GPS SV ephemeris and clock errors are highly correlated, and a large percentage of these error contributions cancels in all of these cases. Therefore, the uncorrelated receiver clock errors are the primary contributors to the relative navigation error for this formation. For two MEO satellites separated by approximately 10 kilometers, the Monte-Carlo simulations yielded a steady-state time-wise ensemble RMS relative accuracy of approximately 0.43 meters in position and 0.25 millimeters per second in velocity, with maximums below 2.2 meters in position and 1.4 millimeters per second in velocity. The relative accuracy is well within the 100-meter and 20-millimeter-per-second mission requirements for a 10-kilometer separation. During a 1-day prediction using a converged filter solution, the relative errors remain under 9 meters in position and 8.5 millimeters per second in velocity.

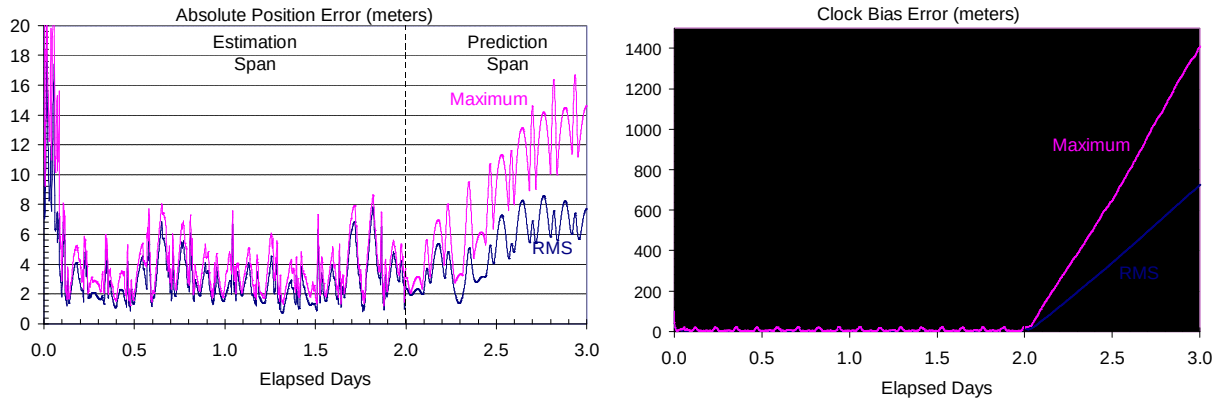

Figure 5. Ensemble Absolute Position and Clock Bias Errors for MEO Formation Using Independently-Estimated Solutions with Standard GPS Measurements

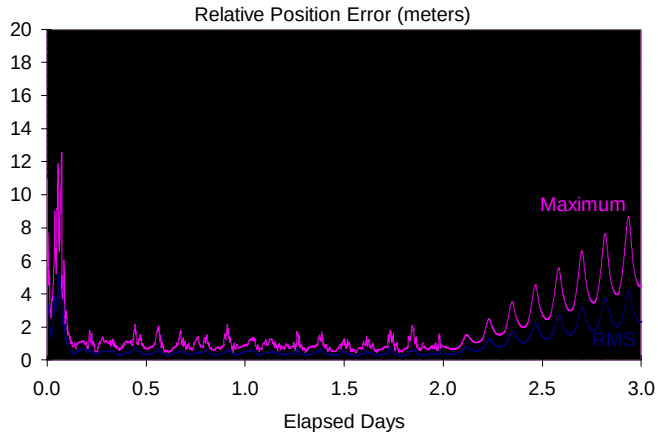

Figure 6. Ensemble Relative Position Errors for MEO Formation Using Independently-Estimated Solutions with Standard GPS Measurements

Simulations were performed to evaluate the relative performance of the navigation algorithms listed in Table 1, using a representative measurement set from the Monte Carlo simulation. Table 4 compares the steady-state absolute error statistics for the local satellite for each of the navigation algorithms evaluated. Table 5 compares the steady-state relative error statistics for the local satellite and one remote satellite for each of the navigation algorithms evaluated. The variation in the absolute error statistics for all satellites in the formation is about 5 percent. The variation in the relative error statistics for all satellites in the formation is less than 30 percent. These comparisons produced the following results:

- Simultaneously estimating the local and remote satellites produced identical absolute and relative results to those obtained by independently estimating each of the satellites.
- Estimation of a pseudorange bias for each GPS SV can be used to absorb much of the unmodeled ionospheric delay errors producing smoother clock bias estimates. However, due to the high correlation between the pseudorange and clock biases, the clock state improvement is very sensitive to the initial pseudorange bias value that is used and the process noise parameters used for the clock bias and pseudorange bias. When tuned to provide improved clock bias estimates, the absolute navigation position and velocity errors increased significantly and the relative navigation errors increased slightly as compared with the case where the biases were not estimated. In this analysis, the pseudorange bias was modeled as a

random walk variable; better absolute results might be achieved if the pseudorange bias model better reflected the physical characteristics of the expected ionospheric delay.

- When only singly-differenced GPS measurements were processed, the absolute state vector solutions were unstable. The inclusion of standard GPS measurements for only the local satellite in addition to singly-differenced GPS pseudorange measurements between the remote and local satellites stabilized the absolute solutions, yielding absolute navigation accuracy comparable to the processing of only standard GPS measurements. However, the relative navigation errors increased due to the less-complete cancellation of the standard GPS measurement errors. The magnitude of this increase was found to be sensitive to the relative weighting of the two measurement types, with equal weighting producing the smallest relative error.
- Inclusion of 1-way (remote-to-local) intersatellite pseudorange in addition to standard GPS pseudorange measurements for the remote and local satellites did not improve the absolute navigation results obtained without the 1-way measurements. In this case, the relative navigation errors increased by about 5 percent.
- Inclusion of roundtrip intersatellite range between the local and remote satellites in addition to standard GPS pseudorange measurements for the remote and local satellites produced comparable absolute results to those obtained without the round-trip measurements. However, the relative navigation errors decreased by about 25 percent due to a reduction in the impact of the uncorrelated receiver clock biases associated with the standard GPS measurements.

Table 4. Steady-State Absolute Error Statistics for the MEO Formation

Navigation Algorithm	Position Error (meters)		Velocity Error (millimeters per second)		Clock Error (meters)	
	RMS	Maximum	RMS	Maximum	RMS	Maximum
Independent	3.36	8	1.7	5.8	8.0	25
Simultaneous with standard GPS	3.36	8	1.7	5.8	8.0	25
Simultaneous with standard GPS and bias estimation	13.8	23	5.9	12.6	6.7	20
Simultaneous with standard and differenced GPS	3.52	9	1.7	5.7	8	24
Simultaneous with standard GPS and 1-way intersatellite pseudorange	3.37	8	1.7	5.8	8	25
Simultaneous with standard GPS and round-trip intersatellite range	3.36	8	1.7	5.9	8	25

Table 5. Steady-State Relative Error Statistics for the MEO Formation

Navigation Algorithm	Position Error (meters)		Velocity Error (millimeters per second)	
	RMS	Maximum	RMS	Maximum
Independent	0.42	1.3	0.25	0.93
Simultaneous with standard GPS	0.42	1.3	0.25	0.93
Simultaneous with standard GPS and bias estimation	0.66	2.1	0.34	1.01
Simultaneous with standard and differenced GPS	0.71	2.4	0.40	1.17
Simultaneous with standard GPS and 1-way intersatellite pseudorange	0.45	1.4	0.26	1.06
Simultaneous with standard GPS and round-trip intersatellite range	0.31	0.8	0.18	0.60

5 – RELATIVE NAVIGATION PERFORMANCE FOR HIGH ALTITUDE FORMATION

This section presents the absolute and relative navigation results for the HEO formation. Figure 7 illustrates the geometry of the HEO spacecraft with respect to the primary and first side lobe of the signal of a single GPS SV (ignoring the effects of the differences in inclinations). The formation is above the GPS constellation and outside the primary beam for a large portion of its orbit.

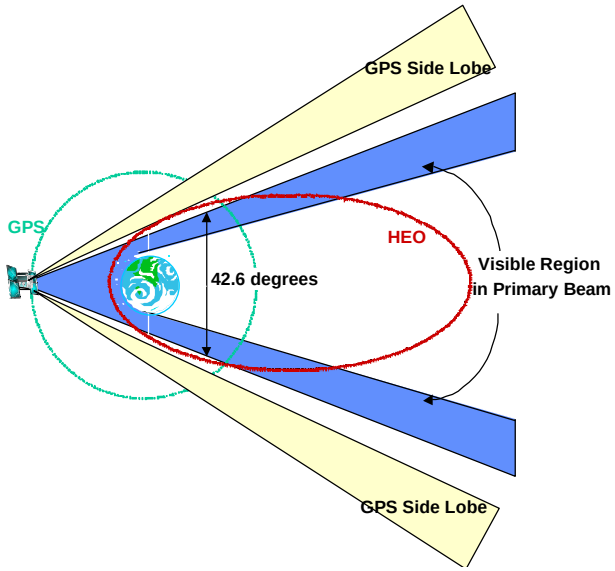

Figure 7. HEO Tracking Geometry

Figure 8 shows the number of GPS SVs that can be acquired and tracked by a GPS receiver on a 1.2x12 Earth-radii HEO, assuming a 30-dB-Hertz receiver acquisition and tracking threshold. This reduced threshold was selected because preliminary analysis performed using a receiver with a standard 35-dB-Hertz threshold did not meet the relative navigation requirements for the initial phase of the MMS mission. The 30-dB-Hertz tracking threshold can be achieved if the receiver employs weak signal tracking strategies to track the weaker signals in the side lobes of the GPS antenna pattern (Reference 7). In this case, the receiver can acquire and track at least one GPS SV about 27 percent of the time and can acquire a maximum number of 22 GPS SVs at perigee. The HEO receiving antenna model consists of two hemispherical antennas, one located on the top face of the satellite and one located on the bottom face. Use of a nadir-pointing high gain GPS antenna would further improve GPS signal acquisition and tracking at high altitudes.

Figure 9 shows the ensemble RMS and maximum absolute position and clock bias errors for the local satellite over the 3.5-day estimation time span followed by a 1-day prediction time span, from Monte Carlo simulations in which all satellites were independently estimated using standard GPS measurements. The estimation process reached steady state immediately following the first perigee passage. The steady-state time-wise ensemble RMS of the absolute errors were 75 meters position, 3.8 millimeters per second velocity, and 49 meters (0.16 microseconds) clock bias, which were consistent with the state errors predicted by the estimator. The maximum errors occur following apogee. The absolute position accuracy is well within the 100-kilometer mission requirement. The maximum absolute errors encountered were less than 365 meters in position, 27 millimeters per second in velocity, and 265 meters (0.88 microseconds) in clock bias. The primary sources of the absolute navigation error are dynamic modeling errors, unmodeled ionospheric delay, and receiver clock errors. During a 1-day prediction using a converged filter solution, the absolute errors remain under 3.3 kilometers in position, 2.3 meters per second in velocity, and 400 meters (1.3 microseconds) in clock bias for all Monte Carlo cases that were run.

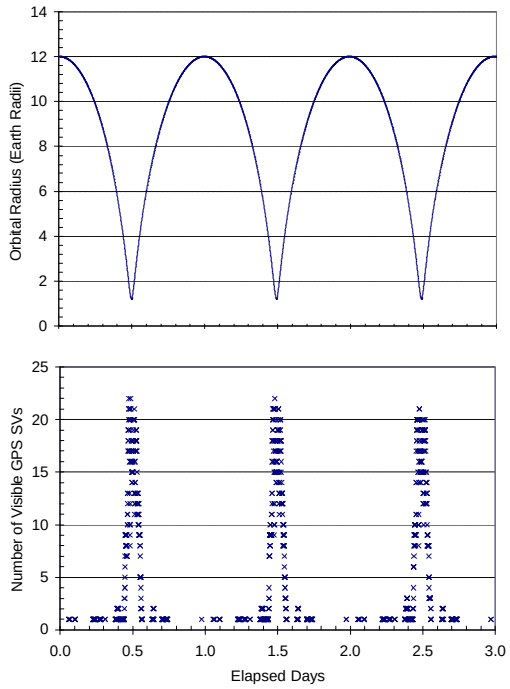

Figure 8. GPS SV Visibility as a Function Time and Altitude for HEO Formation

Figure 10 shows the ensemble RMS and maximum relative position errors for the local satellite and one remote satellite, from Monte Carlo simulations in which all satellites were independently estimated using standard GPS measurements. The dynamic modeling errors and ionospheric errors will nearly cancel when the absolute state vectors are differenced. In addition, since the satellites are in close formation and track common GPS SVs 98.7 percent of the time, the ionospheric delay and GPS SV ephemeris and clock errors are highly correlated, and a large percentage of the these error contributions cancels in all of these cases. Therefore, the uncorrelated receiver clock errors are the primary contributors to the relative navigation error for this formation. For this HEO satellite formation, the Monte-Carlo simulations yielded a steady-state time-wise ensemble RMS relative position accuracy of approximately 76 meters, with a maximum below 400 meters. During a 1-day prediction using a converged filter solution, the relative errors remain under 3.4 kilometers in position and 2.3 meters per second in velocity.

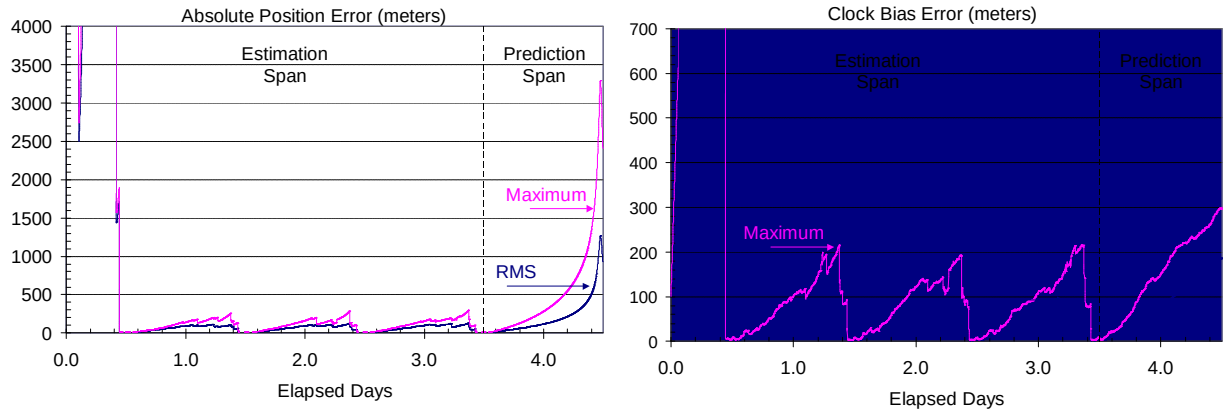

Figure 9. Ensemble Absolute Position and Clock Bias Errors for HEO Formation Using Independently-Estimated Solutions with Standard GPS Measurements

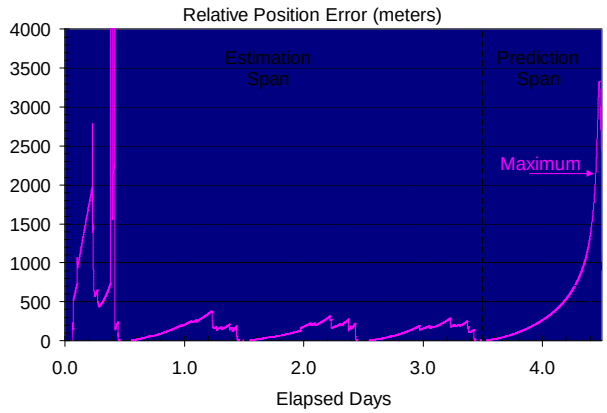

Figure 10. Ensemble RMS and Maximum Relative Position Errors for HEO Formation Using Independently-Estimated Solutions with Standard GPS Measurements

Additional Monte-Carlo simulations were performed to evaluate the relative performance of several of the navigation algorithms listed in Table 1. Tables 6 and 7 compare the steady-state time-wise ensemble absolute and relative error statistics for each of the navigation algorithms evaluated, respectively. The statistics listed are the largest errors obtained for all satellites in the formation. . The variation in the error statistics for all satellites in the formation is less than 10 percent for the absolute errors and 50 percent for the relative errors. These comparisons produced the following results:

- Simultaneously estimating the local and remote satellites produced identical absolute and relative results to those obtained by independently estimating each of the satellites.
- Inclusion of singly-differenced GPS pseudorange measurements between the remote and local satellites in addition to standard GPS measurements for the local satellite produced a small increase in the absolute errors. The relative navigation errors increased by about 10 percent due to less complete cancellation of the standard GPS measurement errors.
- Inclusion of 1-way (remote-to-local) intersatellite pseudorange in addition to standard GPS pseudorange measurements for the remote and local satellites produced comparable absolute and relative results to those obtained without the 1-way measurements.
- Inclusion of round-trip intersatellite range between the local and remote satellites in addition to standard GPS pseudorange measurements for the remote and local satellites produced a significant reduction in both the absolute and relative navigation errors (Figures 11 and 12) due to a reduction in the impact of the uncorrelated receiver clock biases associated with the standard GPS measurements.

Table 6. Steady-State Time-Wise Ensemble Absolute Error Statistics for the HEO Formation

Navigation Algorithm	Position Error (meters)		Velocity Error (millimeters per second)		Clock Error (meters)	
	RMS	Maximum	RMS	Maximum	RMS	Maximum
Independent	75	365	3.8	27	49	265
Simultaneous with standard GPS	75	365	3.8	27	49	265
Simultaneous with standard and differenced GPS	76	442	3.9	27	51	297
Simultaneous with standard GPS and 1-way intersatellite range	76	351	4.0	26	48	266
Simultaneous with standard GPS and round-trip intersatellite range	56	182	2.8	20	31	136
Simultaneous with standard GPS and round-trip intersatellite range (with 35-db_Hertz threshold)	134	1045	7.5	76	79	413

Table 7. Steady-State Time-Wise Ensemble Relative Error Statistics for the HEO Formation

Navigation Algorithm	Position Error (meters)		Velocity Error (millimeters per second)	
	RMS	Maximum	RMS	Maximum
Independent	76	391	4.1	30
Simultaneous with standard GPS	76	391	4.1	30
Simultaneous with standard and differenced GPS	81	517	4.5	39
Simultaneous with standard GPS and 1-way intersatellite pseudorange	76	485	4.2	36
Simultaneous with standard GPS and round-trip intersatellite range	24	117	1.3	6.2
Simultaneous with standard GPS and round-trip intersatellite range (with 35-db_Hertz threshold)	19	101	1.2	6.3

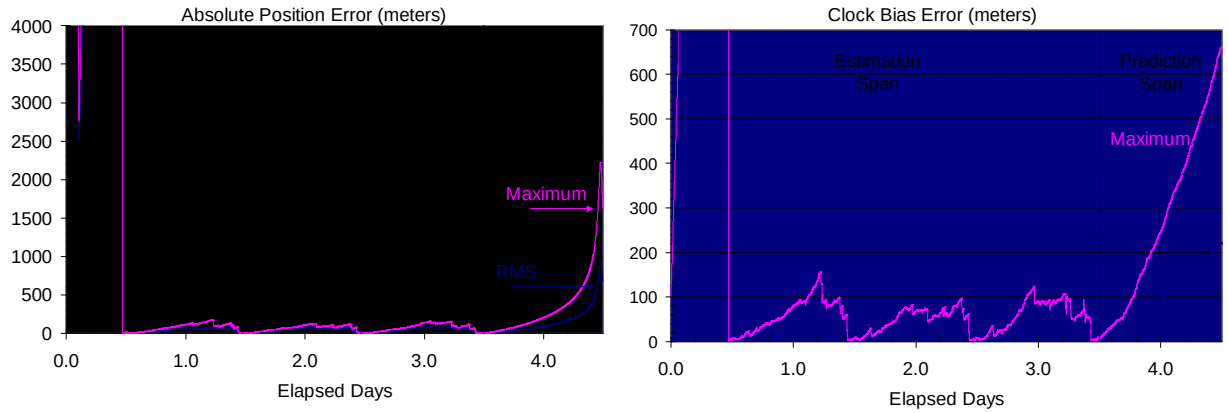

Figure 11. Ensemble Absolute Position and Clock Bias Errors for HEO Formation Using Simultaneously-Estimated Solutions with Standard GPS and Round-Trip Intersatellite Measurements

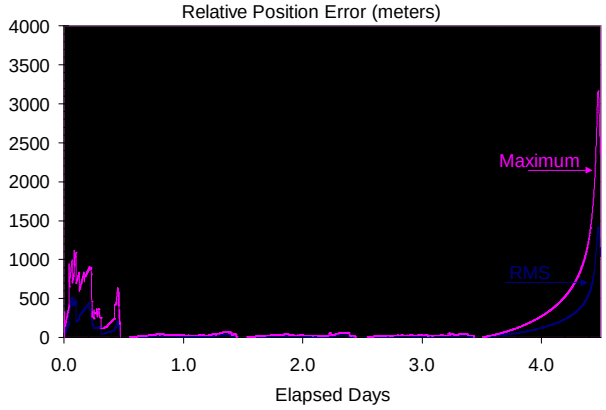

Figure 12. Ensemble RMS and Maximum Relative Position Errors for HEO Formation Using Simultaneously-Estimated Solutions with Standard GPS and Round-Trip Intersatellite Measurements

Because of the improvement obtained by including round-trip intersatellite range, the navigation performance was investigated that could be achieved by processing round-trip intersatellite measurements in addition to GPS measurements from a more standard space receiver with a 35-dB-Hertz tracking and acquisition threshold. Reduction in the number of standard GPS measurements increased the absolute navigation errors but the relative navigation errors decreased due to a reduction in the impact of the uncorrelated receiver clock biases associated with the standard GPS measurements.

6 – CONCLUSIONS AND FUTURE DIRECTIONS

This study assessed the relative navigation accuracy achievable using a high-accuracy multi-satellite filter to simultaneously estimate the satellite state vectors for a 500x7000 kilometer altitude MEO and a 1.2x12 Earth radii HEO formation. The satellites in both formations are in nearly co-planar orbits with intersatellite separations sufficiently small that the satellites acquire and track the same GPS SVs more than 98.5 percent of the time Improvements to be achieved through the estimation of GPS biases, differencing of GPS measurements, and addition of intersatellite range measurements were evaluated..

For both formations using only GPS measurements:

- The frequency of acquisition and tracking of signals from common GPS SVs was found to be the primary factor driving the relative navigation accuracy.
- The quality of the receiver clocks was found to be the next largest contributor to the relative navigation error.
- Comparable absolute and relative navigation accuracies were obtained using absolute state vectors estimated either independently or simultaneously based on standard GPS pseudorange measurements.
- GPS bias estimation was found to improve clock estimation in some cases but did not improve the relative navigation performance.
- The processing of only singly-differenced GPS measurements did not provide a stable absolute solution. The processing of singly-differenced GPS measurements in combination with standard GPS pseudorange to the local satellite did not provide any accuracy improvement. Their use may be more appropriate for a relative filter that uses the estimated trajectories from independent filters as reference trajectories.

For the MEO formation, which has nearly continuous tracking of the GPS signals, the differencing of absolute state vectors can provide a relative navigation accuracy of better than 2.5 meters in position and 1.5 millimeters per second in velocity. For the HEO formation, which has continuous tracking of the GPS signals only near perigee, the differencing of absolute state vectors can provide a relative navigation accuracy of better than 400 meters in position and 30 millimeters per second in velocity, using a GPS receiver with weak signal tracking improvements and a highly stable clock.

For these close formations when only GPS measurements were processed, the operationally-more-complex simultaneous estimation algorithm did not provide any accuracy benefit over the operationally-simpler and more efficient approach of differencing independently-estimated state vectors. This conclusion appears to be in conflict with the following results achieved in real and simulated flight demonstrations using real measurements provided by GPS receivers:

- Flight data results published by one of the authors (Reference 10) show superior performance of a simultaneous estimator that estimated common measurement biases. However, that conclusion was based on the assumption of zero correlation of the absolute errors in the independently-estimated solutions, a very conservative assumption corresponding to the case in which the receivers are tracking no common GPS SVs. For the formations studied in this paper, which can track the same GPS SVs more than 98.5 percent of the time, much higher cancellation of the absolute errors would be expected.
- Reference 11 evaluated relative navigation performance using two GPS receivers running in a simulated flight environment. In that experiment, a simultaneous estimator that processed pseudorange measurements from only common GPS SVs provided superior performance as compared with differencing independently-estimated state vectors computed using all available measurements from each receiver. The author concluded that the poorer performance of the latter method was primarily because a significant number of measurements from uncommon GPS SVs were processed in the independent estimators.

Comparison of the results presented in the current paper with the real and simulated flight data results shows the sensitivity of the relative navigation accuracy to the percentage of measurements from common GPS SVs that are processed, a result the authors also demonstrated in Reference 4. The real data results point out that even though all satellites in the formation may be able to acquire and track a very high percentage of common GPS SVs, the actual

percentage of common SVs tracked may be significantly smaller. In a real flight environment, it will be difficult to synchronize independent estimators running on each satellite in the formation to process measurements from only common GPS SVs. The processing of measurements from only common GPS SVs can be better controlled using a simultaneous estimation algorithm.

For both formations, the inclusion of accurate round-trip intersatellite range measurements in the simultaneous estimation algorithm was found to improve relative navigation accuracy by reducing the impact of the GPS receiver clock biases. For the HEO formation, the inclusion of accurate round-trip intersatellite range was found to significantly improve both absolute and relative navigation accuracy. However, it should be noted that the results presented for round-trip intersatellite range are optimistic with respect to the elimination of all biases on the round-trip range.

Future directions will focus on the navigation performance that can be achieved using less accurate clocks, a more detailed investigation of the navigation accuracy that can be achieved by including intersatellite measurements, and investigations of formations flying in different orbital configurations. The relative navigation version of GEODE will be integrated into a low cost GPS satellite receiver being developed by the GSFC GNCC. This formation-flying receiver will be used to demonstrate end-to-end performance in GNCC's formation-flying test bed.

ACKNOWLEDGEMENTS

This research was supported by the NASA Space Operations and Management Office and NASA Research Announcement 98-OSS-10: Technology Development for Explorer Missions.

REFERENCES

1. C. Gramling et al., "Preliminary Operational Results of the TDRSS Onboard Navigation System (TONS) for the Terra Mission," Paper MS00/32, *Proceedings of the International Symposium on Space Dynamics*, CNES, Biarritz , France, June 26-30, 2000
2. R. Hart, A. Long, and T. Lee, "Autonomous Navigation of the SSTI/Lewis Spacecraft Using the Global Positioning System (GPS), *Proceedings of the Flight Mechanics Symposium 1997*, NASA Conference Publication 3345, May 19-21, 1997, pp.123-133
3. F. Bauer et al., "Enabling Spacecraft Formation Flying Through Spacebourne GPS and Enhanced Autonomy Technology," *Proceedings of the ION GPS-99*, Nashville, TN, September 1999.
4. A. Long et al., "Autonomous Relative Navigation for Formation-Flying Satellites Using GPS," Paper MS00/18, *Proceedings of the International Symposium on Space Dynamics*, CNES, Biarritz , France, June 26-30, 2000.
5. J. R. Carpenter, "A Preliminary Investigation of Decentralized Control for Satellite Formations," Paper 264 presented at the IEEE Aerospace Conference, Big Sky Montana, March 20-22, 2000.
6. Goddard Space Flight Center, CSC-96-968-01R0UD3, *Global Positioning System (GPS) Enhanced Orbit Determination (GEODE) Mathematical Specifications, Version 5*, T. Lee and A. Long (CSC), prepared by Computer Sciences Corporation, February 2001.
7. M. Moreau et al., "GPS Receiver Architecture and Expected Performance for Autonomous GPS Navigation in High Earth Orbits," *NAVIGATION: Journal of the Institute of Navigation,* Vol. 47, No. 3, Fall 2000, pp. 191-204.
8. Johnson Space Center, *Range Bias Models for GPS Navigation Filters*, William M. Lear, Charles Stark Draper Laboratory, June 1993.
9. R. G. Brown and P. Y. C. Hwang, *Introduction to Random Signals and Applied Kalman Filtering*, Third Edition, John Wiley and Sons, 1997.
10. J. R. Carpenter and E. R. Schiesser, "Semi-Major Axis Knowledge and GPS Orbit Determination," accepted for publication in *NAVIGATION: Journal of the Institute of Navigation*.
11. P. W. Binning, *Absolute and Relative Satellite to Satellite Navigation Using GPS*, Ph.D. Dissertation, Colorado Center for Astrodynamics Research, University of Colorado, May 1997